Flow, Turbulence and Combustion
https://doi.org/10.1007/s10494-025-00638-7

RESEARCH

On the Impact of CFD Turbulence Models for Premixed NH_3/H_2 Combustion on Emissions and Flame Characteristics in a Swirl-Stabilized Burner

Luca Mazzotta[1,2] · Rachele Lamioni[3] · Giuliano Agati[4] · Adriano Evangelisti[1] · Franco Rispoli[4] · Agustin Valera-Medina[5] · Domenico Borello[4]

Received: 28 May 2024 / Accepted: 17 January 2025

Abstract
Ammonia combustion is gaining interest as a feasible alternative to traditional fossil fuels because of to the low environmental impact and as hydrogen and energy carrier. This study used Computational Fluid Dynamics (CFD) simulations to compare various turbulence models for premixed ammonia/hydrogen combustion in a swirl-stabilized burner. The primary aim was to identify the best turbulence model for accurately predicting the flow dynamics, combustion behaviour, and emissions profiles of ammonia/hydrogen fuel blends. The turbulence models evaluated were Large Eddy Simulation (LES), Realizable k-ϵ, Renormalization Group (RNG) k-ϵ, k-ω SST, and Reynolds Stress Model (RSM). On the LES side, a further comparison of two subgrid models (Smagorinsky-Lilly and WALE) was investigated. The Flamelet Generated Manifold (FGM) method was utilized with a detailed chemistry scheme taking into consideration all NO_x reactions. To improve the prediction of NO_x emissions, additional scalar transport equations for NO and NO_2 were included. This methodology aimed to be a balance between computational efficiency and the accuracy expected of detailed chemistry models. Validation was done with a swirl burner from Cardiff University's Gas Turbine Research Centre. Results showed that all turbulence models accurately captured flame characteristics in terms of exhaust temperature and axial velocity with minor differences in the recirculation zones, where only the RSM model can predict the velocity trend as the LES simulation while other RANS models differ by at least 7 m/s. The temperature reached by the LES resulted 100 K higher than the other models in the flame zone. LES simulation can predict the emission value with an error of less than 10%. Moreover, the error related to emissions derived from the RANS simulations was not negligible, underestimating NO_x emissions by about 35%. However, RSM model produced results that were closer to those derived from the high-fidelity LES when compared to the others RANS models, particularly in terms of flame thickness and emissions. It was concluded that it is mandatory to perform an unsteady analysis to reach reasonable results.

Keywords Ammonia · Hydrogen · NOx · Large eddy simulation · Gas turbine

Extended author information available on the last page of the article

1 Introduction

The rising requirements for renewable energy sources has increased interest in hydrogen as a viable option for both power generation and transportation (Valera-Medina et al. (2018); Mashruk et al. (2024)). On the other hand, using hydrogen as a fuel involves several technical challenges, in particular NO_x emissions over the allowed limit (Li and Li (2021); Ilbas et al. (2005)). A promising way for overcoming these challenges involves leveraging ammonia (NH_3) as a hydrogen carrier due to its abundant availability, high hydrogen content, and low carbon footprint (Kobayashi et al. (2019)). Accurately predicting NO_x emissions from ammonia combustion requires sophisticated chemical models that integrate detailed reaction mechanisms with transport phenomena (Xiao and Valera-Medina (2017)). These models capture the formation and destruction pathways of NO_x, influenced by local temperature and pressure conditions. Coupling chemical kinetics with computational fluid dynamics (CFD) allows for high-fidelity simulations that provide spatial and temporal resolution of the combustion process. To effectively optimize the combustion of ammonia/hydrogen mixtures, it's crucial to understand the intricate interaction between turbulence, chemistry and emissions during the combustion process (Safavi and Amani (2018)). Even if swirled burners are frequently used in power generation (Chiong et al. (2021)), their complex swirling flow patterns pose difficulties in predicting flow and combustion behaviors using simple models. Computational Fluid Dynamics (CFD) simulations have emerged as useful tools for studying ammonia/hydrogen combustion in swirl-stabilized burners. Selecting the appropriate turbulence model is crucial for achieving the required accuracy in CFD simulations, which regulate the turbulence effects on flow characteristics and combustion dynamics. In addiction, the prediction of NO_x emissions from the combustion of high-hydrogen content mixtures is still challenging, particularly when combined with ammonia, and efforts are currently ongoing to obtain a chemical kinetics model suitable for predicting and evaluate emissions with negligible error (da Rocha et al. (2019), Alnasif et al. (2023)). Füzesi et al. (2024) have demonstrated the feasibility of estimating NO_x emissions using surrogate models to reduce computational costs. However, high-fidelity turbulence-chemical interaction models like the Eddy Dissipation Concept (EDC) model proposed by Magnussen (1976), despite allowing accurate results with limited calibration, demands significant computational resources. The same combustion model was tested by Mazzotta et al. (2024), where the effect of pressure on NO_x emission was investigated; although the emissions were found to have an error of less than 3%, the combustion model was extremely time-consuming. Therefore, the need to obtain acceptable results with a simplified combustion model emerged. Within this context, the Flamelet Generated Manifold (FGM) model introduced by Oijen and Goey (2000) along with solving additional scalar transport equations for NO_x offers a promising approach to reducing computational costs in turbulent combustion simulations, only enhancing the accuracy of transported species of special interest. This paper conducts a comparative examination of various turbulence models such as Large Eddy Simulation (LES), Realizable and RNG k-ϵ, k-ω SST and Reynolds Stress Model (RSM) for simulating ammonia/hydrogen combustion in a swirl-stabilized burners. The burner utilized in Cardiff University's Gas Turbine Research Centre was used as a validation test case. The primary goal of this study was to compare and evaluate the accuracy of these turbulence models in simulating ammonia/hydrogen combustion, determining the most suitable models for this type of application while balancing computational time and error for the parameters investigated. The analysis of these numerical models aims to analyse the intricate interactions between the

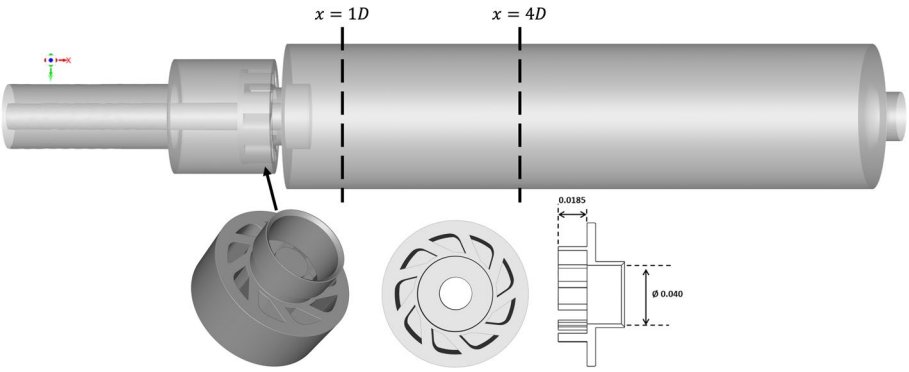

Fig. 1 Computational domain investigated of the HPGSB/HPOC (upper). Detailed geometry of radial-tangential swirler/burner nozzle insert (bottom). Dimensions in meters

combustion process, turbulence, and emissions where experimental measurements cannot provide sufficient information, through an investigation in an innovative burner with mixtures of relevant interest that have not been adequately studied in the literature. According to the authors' knowledge, no equivalent studies have been conducted under the considered operating conditions.

2 Numerical Setup

2.1 Test Facility, Computational Domain and Operating Conditions

The validation test case and computational domain selected for the present numerical investigation was the swirl burner located in the Cardiff University's Gas Turbine Research Centre (GTRC).[1] This burner was situated within the high pressure optical chamber (HPOC). The HPOC configuration had a cylindrical quartz burner confinement, facilitating optical access to the flame for observation and analysis. A sufficient inlet length was provided to allow the flow to fully develop before entering the combustion chamber. Figure 1 shows the detailed view of the computational domain considered of the HPGSB/HPOC and the geometry of the radial-tangential swirler. Previous works (Pugh et al. (2019); Runyon et al. (2018); Mazzotta et al. (2024)) include further information on the design and operation of this high-pressure combustion rig test facility. Exhaust gas was sampled downstream the liner for the measure of emissions. The water content, residual oxygen, unburned NH_3 and NO_x were measured through a bespoke Emerson CT5100 Quantum Cascade Laser analyzer at the frequency of 1 Hz. NO_x measurements were performed in hot and wet conditions using a heated probe. The temperature of the quartz was monitored at several points along the liner, as well as the burner nozzle and dome. These experimental data were utilised to determine the appropriate thermal boundary conditions for the CFD model. The operating conditions were summarized in Table 1; a mixture composed by 75%H_2/25%NH_3 (by vol.) was selected as fuel with dry air as oxidant. Considering the amount of hydrogen in

[1] https://www.cu-gtrc.co.uk.

Table 1 Operating conditions

X_{H_2}	75%
X_{NH_3}	25%
Equivalence ratio, ϕ	0.29
Operating temperature, T_{in}	500 K
Operating pressure, p	1.1 bar
Mass flow inlet, $\dot{m}$	13.28 g/s
Swirl number, S_g	0.8

the mixture, an equivalence ratio of 0.29 was chosen, to maintain an adequate NO_x level. Considering the amount of hydrogen in the mixture considered in this study (75% by vol.), to maintain an adequate level of NO_x emissions, it was decided to operate at an equivalence ratio that would allow the lowest possible NO_x emissions, while keeping the flame stable, avoiding lean blow-off conditions. The preliminary analysis to obtain a suitable equivalence ratio was carried out in a previous work (see Fig. 6 in Mazzotta et al. (2024)). More precisely, an equivalence ratio of 0.29 was chosen. The operating temperature and pressure were assumed equal to 500K and 1.1 bar, respectively. The swirler was characterized by a swirl number, $S_g = 0.8$. The wall temperatures were imposed according to thermocouples measurements derived by experimental campaign and shown by Mazzotta et al. (2024). Zero diffusive flux species and no-slip boundary condition were employed at the wall. The solid wall material of the combustor was realized in quartz.

2.2 Mesh Resolution

A three-dimensional (3D) computational domain was employed to model the geometry of the HPGSB burner. Two distinct meshes have been established, one for the RANS simulations and one for the LES consisting in 3.4×10^6 and 8.7×10^6 polyhedral cells, respectively. Figure 2 shows a detailed section of the computational grid used for the LES. A fine mesh resolution was used for the swirler, nozzle and flame zone sections, given the significant variations in physical variables, while the rest of the combustor was characterized by a coarser mesh. The flame zone region was further locally refined

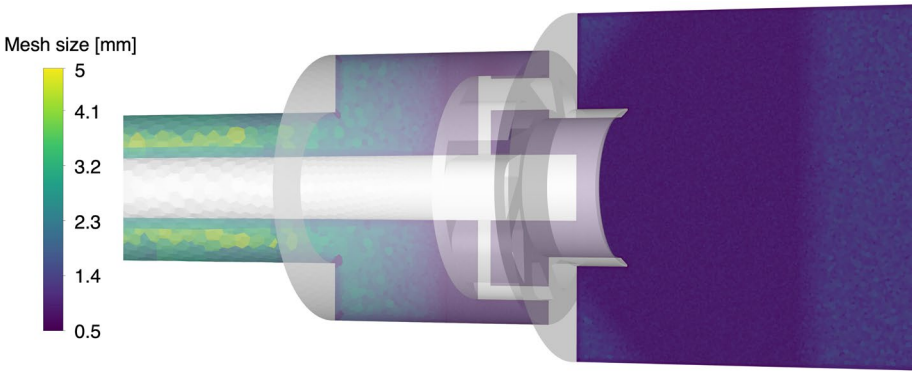

Fig. 2 Cell size distribution adopted in the computational domain for the spatial discretization, used for the LES

to better capture the combustion process. The same approach in terms of refinement was used for the RANS mesh. To be sure that the adopted grid was able to solve more than 80% of the turbulent length scales for high quality LES, according with Pope's criterion (Pope (2000, 2004)), Eq. (1) was applied at the operating conditions.

$$l_{sgs} = l_0[(1-\epsilon) + \epsilon Re_t^{-1/2}]^{3/2} \tag{1}$$

where l_0 was the integral length scale, ϵ was the turbulence dissipation rate and Re_t was the turbulent Reynolds number. In Fig. 3, an assessment of the Pope's criterion was shown; the subgrid scale turbulent kinetic energy, k_{sgs}, was evaluated using Eq. 2.

$$k_{sgs} = \frac{1}{C_{DS}} \frac{v_{sgs}}{\rho \Delta^{1/3}} \tag{2}$$

where C_{DS} was the subgrid scale dynamic-Smagorinsky viscosity constant, ρ was the density of the mixture, Δ was the characteristic length and v_{sgs} was the subgrid scale viscosity. Although a detailed grid sensitivity analysis was not conducted due to the high computational cost, the cell size of the RANS mesh was estimated using information derived from previous studies (Mazzotta et al. (2024)) in which a detailed grid sensitivity analysis was conducted, maintaining the same level of refinement as previously used, thus ensuring sufficient resolution in critical regions. On the LES side, the grid employed in this study was carefully designed to resolve more than 90% of the turbulent length scales, as per Pope's criterion (see Fig. 3). In particular, a cell size of 0.5 mm was used in the flame zone and the swirler zone, while in the remaining zones a cell size gradually increased to 1 and 2 mm. The inlet zone is characterized by a cell size of 3-5 mm given the unnecessary refinement. This approach is consistent with established practices in the literature for the same configuration used, as demonstrated in studies such as Ouali (2024); Meloni et al. (2023); Castellani et al. (2023); Ansari et al. (2024); Meloni et al. (2024); Castellani et al. (2024); Mashruk et al. (2023). The resolution adopted ensures adequate accuracy in capturing the critical features of the flow and combustion processes investigated. Furthermore, the aspect ratio and skewness values were carefully checked to be sure of the accuracy of the mesh.

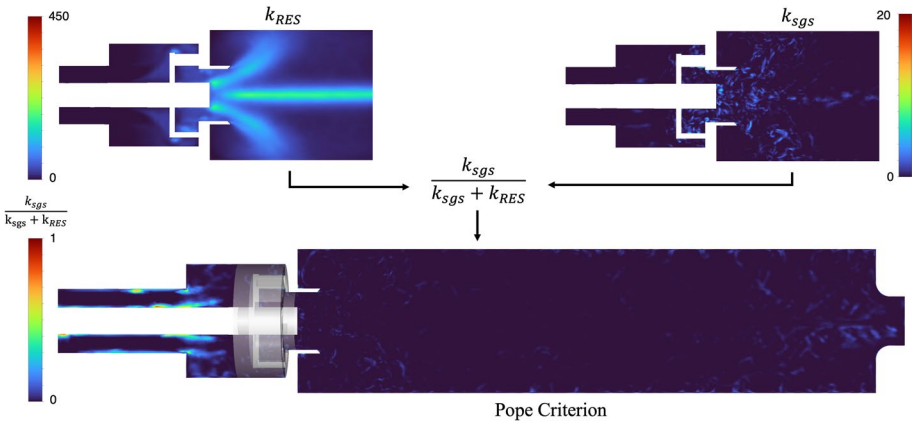

Fig. 3 Pope criterion assessment to evaluate mesh quality

Specifically, the skewness value is always less than 0.83 with an average value of less than 0.32. Regarding the aspect ratio, the maximum value is 4.1.

2.3 Numerical and Combustion Models

The numerical results reported in this work were obtained using the commercial CFD code Ansys Fluent 22R2. Both steady-state Reynolds-Averaged Navier–Stokes (RANS) and Large Eddy Simulation (LES) turbulence models were compared for the purpose of this work and listed in Table 2.

On the RANS side, most of the turbulence models available in Ansys Fluent were compared. Specifically, the Realizable k-ϵ (Wilcox (1998)), RNG k-ϵ (Yakhot et al. (1992)), k-ω SST (Menter (1994)) and Reynolds Stress (RSM) (Hanjalić and Launder (1972)) models. On the LES side, two different model was compared: the Smagorinsky-Lilly model (Smagorinsky (1963)) with Dynamic Subgrid-scale (Germano et al. (1991)), named here as *DSL*, and the Wall-Adaptive Local Eddy Viscosity (WALE)(Nicoud and Ducros (1999)) model were employed at the turbulence subgrid scale for a further comparison from the perspective of high-fidelity models. The ideal gas law was used to model the working fluid as a compressible medium. This approach accounts for the density variations as a function of temperature, along with minimal but present pressure drops. Both spatial and implicit temporal discretization were solved with Second-Order Upwind scheme, while the SIMPLE scheme for pressure–velocity coupling was used. The extra transport equations for NO and NO_2 were also solved with the Second-Order approach. For the LES, the time-step size remains constant throughout the simulation. Its value was 2.5×10^{-5} s to keep the Courant-Friedrichs-Lewy number below unity across the domain, particularly in the flame zone region where velocity reaches its peak. A preliminary wash-out phase including 4 Flow Through Time (FTT) was carried out. After that, 6 Flow Through Time of the burner were simulated to collect statistics. Regarding RANS, the COUPLED algorithm was considered to achieve the pressure–velocity coupling. The Second-Order Upwind scheme was used for the discretization of the spatial terms, as well as the LES. Quadratic Pressure-Strain Model was used in the Reynolds Stress Model since has been demonstrated to give superior performance in swirled (or rotating) flows (Yang et al. (2003)). In all simulations, the values for Energy Prandtl, Wall Prandtl and PDF Schmidt were all equally set equal to 0.5. A comparison of the Prandtl number values in the computational domain for the two subgrid LES models and the RSM model is shown in the Fig. 4, given the variability of the turbulent Prandtl number in different flow regions, especially in complex turbulent flows. As shown, the WALE model identifies a slightly higher value of Prandtl number than the

Table 2 Turbulence closure models investigated in this work

Type	Model	Temporal discretization	Description
RANS	k-ϵ	Steady-state	2 equations Realizable
RANS	k-ϵ	Steady-state	2-equations RNG
RANS	k-ω	Steady-state	2-equations SST
RANS	Reynolds Stress Model	Steady-state	7-equations Quadratic Pressure Strain
LES	Smagorinsky-Lilly	Transient	Dynamic subgrid-scale
LES	WALE	Transient	Wall-Adaptive Local Eddy

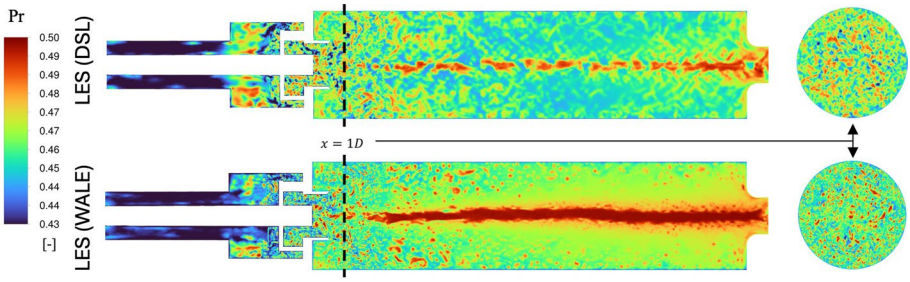

Fig. 4 Instantaneous Prandtl number derived by the two sub-grid LES models (Dynamic Smagorinsky-Lilly and WALE)

Smagorinsky-Lilly model, in particular along the centreline. In the RANS simulations, the values set for the Turbulent Kinetic Energy (TKE) and Turbulent Dissipation Rate (TDR) Prandtl numbers were set equal to 1 and 1.3, respectively. The thermal field was calculated by solving the energy transport equation in the simulations. The thermal boundary conditions imposed on the walls of the chamber were in agreement with the experimental thermocouples values.

The chemistry of the ammonia/hydrogen mixture was modeled using the Flamelet Generated Manifold (FGM) (Van Oijen and de Goey (2000)) approach. The FGM model includes the influence of chemical kinetics on the combustion process, operating under the assumption that combustion can be deconstructed into a series of locally one-dimensional flamelets. These flamelets, representing non-adiabatic premixed laminar flames, were computed using the Cantera (Goodwin et al. (2022)) code. Moreover, the combustion process was characterized by a simplified set of variables, including mixture fraction (Z) and progress variable (c). The progress variable was defined as $c = Y_c/Y_{eq}$, where $Y_c = Y_{N_2} + Y_{H_2O} + Y_{HO_2} - Y_{H_2}$ was the un-normalized progress variable and Y_{eq} was its equilibrium value. Turbulence-chemistry interaction was accounted for by pre-integrating the look-up table with a β - Probability Density Function (β - PDF). The chemical scheme of Otomo et al. (2018) (33 species - 213 reactions) was chosen for the oxidation of ammonia/hydrogen flames, accounting the finite chemistry calculation. The equations related to the mass fraction of NO and NO_2 were solved by additional scalar transport equations. To assess the accuracy of the different turbulence models, the simulated results against experimental NO_x emissions data were compared. Zimont's Turbulent Flame Speed Closure (TFSC) (Zimont et al. (1998); Flohr and Pitsch (2001)) was utilized to characterize the source term for the progress variable, employing a model specifically tailored for wrinkled and thickened flame fronts. The turbulent flame speed expression was calculated by[2]:

$$U_t = A(u')^{3/4} U_l^{1/2} \alpha^{-1/4} l_t^{1/4} \tag{3}$$

where A is the model constant, which was set equal to 0.8 in all simulations carried out in this work, u' was the RMS (root-mean-square) velocity, U_l was the laminar flame speed, α was the unburnt thermal diffusivity and l_t was the turbulent length scale. The turbulent length scale, l_t, for RANS approach was obtained by:

[2] Ansys^{TM} Fluent, Release 22R2, Theory Guide, ANSYS, Inc.

$$l_t = C_D(u')^3/\epsilon \tag{4}$$

where C_D was a model constant equal to 0.37.

With regard to LES, the RANS averaged quantities in the flame speed expression (Eq.(3)) were replaced by their equivalent subgrid quantities; the large eddy length scale, l_t, was defined as:

$$l_t = C_s\Delta \tag{5}$$

where C_s was the Smagorinsky constant, which was set equal to 0.18, and Δ was the characteristic length of the cell. In the WALE model, the calculation of the eddy length scale differs from the Smagorinsky-Lilly one introducing the WALE constant, C_w. In the simulation carried out, C_w was set equal to 0.325. The RMS velocity in Eq.(3) was replaced by the subgrid velocity fluctuation, computed as:

$$u' = l_t\tau_{sgs}^{-1} \tag{6}$$

where τ_{sgs}^{-1} was the subgrid scale mixing rate.

In the Smagorinsky-Lilly model the turbulent viscosity ν_t is given by:

$$\nu_t = (C_s\Delta)^2\sqrt{2S_{ij}S_{ij}}$$

where S_{ij} is the strain rate tensor, defined as:

$$S_{ij} = \frac{1}{2}\left(\frac{\partial u_i}{\partial x_j} + \frac{\partial u_j}{\partial x_i}\right)$$

The WALE model calculates the turbulent viscosity ν_t using a different formulation:

$$\nu_t = (C_w\Delta)^2\frac{\left(S_{ij}^dS_{ij}^d\right)^{3/2}}{\left(S_{ij}S_{ij}\right)^{5/2} + \left(S_{ij}^dS_{ij}^d\right)^{5/4}}$$

where S_{ij}^d is the deviatoric part of the strain rate tensor, calculated as:

$$S_{ij}^d = \frac{1}{2}\left(g_{ik}g_{kj} + g_{jk}g_{ki}\right) - \frac{1}{3}\delta_{ij}g_{kk}$$

The Smagorinsky-Lilly model directly depends on the magnitude of the strain rate tensor, which leads to overestimation of turbulent viscosity in regions of high shear, especially near walls. The WALE model, on the other hand, incorporates both the strain rate and its deviatoric components, allowing it to adapt more accurately to near-wall effects and reduce excessive dissipation, despite being more computationally expensive. However, it can be seen that the WALE model presents a greater challenge since the selection of the constant C_w has the potential to significantly impact the simulation results. Given that this is not a scenario involving a flow with intricate interactions in the vicinity of the wall, the Smagorinsky-Lilly model may be a more suitable option in terms of simplicity and reliability of the results. This article will present a comparison between the two models to evaluate the performance of the two sub-grid models in the context under investigation. The computational time required for each simulation

Table 3 Core hours associated with each turbulence model investigated

Turbulence model	LES (DSL)	LES (WALE)	RSM	k-ϵ Realizable	k-ϵ RNG	k-ω SST
CPU hours [h]	40320	41950	7680	4800	4800	5260

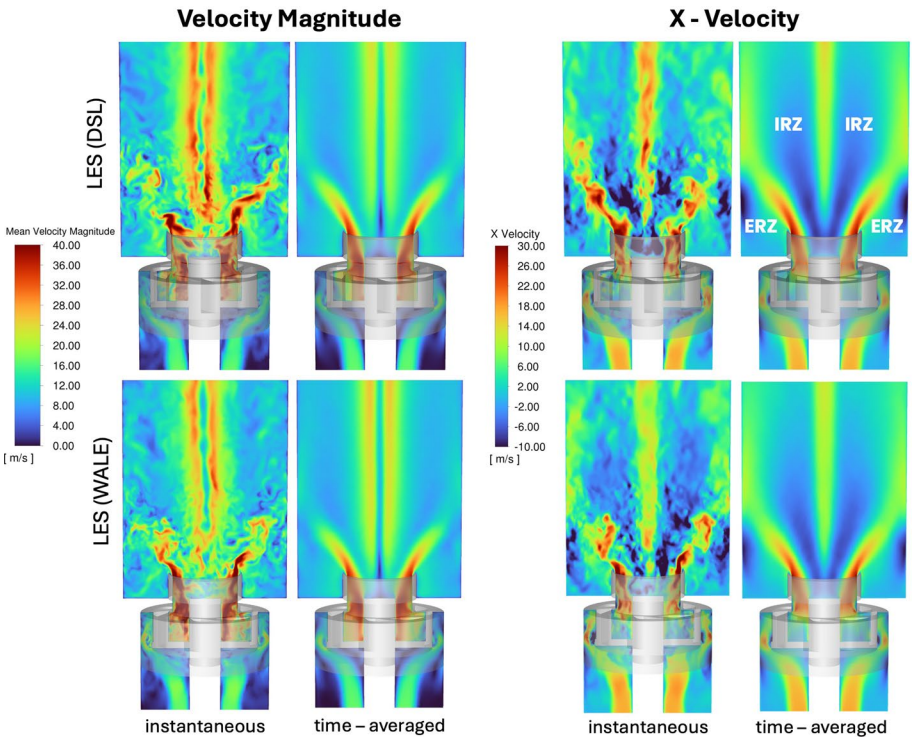

Fig. 5 Instantaneous and time-averaged magnitude and axial velocity fields derived by LES with both Dynamic Smagorinsky-Lilly (DSL) and WALE models

performed in this work is listed in Table 3. The workstation used consists of multiple AMD EPYC 7643 2.3GHz with 512Gb RAM.

3 Results

The comparison of the various models was conducted through an analysis of temperature distribution, velocity profiles, and exhaust emissions. Figure 5 shows the LES instantaneous and time-averaged fields of the velocity magnitude and the axial component using both models employed in this work, namely the Dynamic Smagorinsky-Lilly (DSL) and the WALE models. From the time-averaged fields, it is possible to compare the two different sub-grid models used: no major differences are evident in terms of both magnitude and axial velocity. The axial velocity contour was useful for the quantification of the two recirculation zones given by the tangential swirler, namely the Inner Recirculation Zone

(IRZ) and the External Recirculation Zone (ERZ). The two zones were represented within the time-averaged axial velocity contour. It can be seen that the internal recirculation prevails over the external in terms of volume. The flow was divided by an axial zone along the central axis of the burner, dividing the IRZ into two separate recirculation areas. Inside the IRZ, all hot gases circulate and NO formation takes place. Due to the low calorific value of ammonia and the condition of premixed combustion (in which no stoichiometric condition occur due to diffusion), the mechanisms for NO formation were not predicted by the Zeldovich route (Zeldovich (1946)), where temperatures need to reach temperatures above 1850 K, especially in the flame front. The main mechanism of NO and NO_2 formation was fuel-bound NO_x, due to the significant amount of nitrogen in the fuel mixture.

The LES instantaneous and time-averaged temperature fields and the iso-surface of the progress variable coloured with the temperature, derived by the Dynamic Smagorinsky-Lilly model, are shown in Fig. 6. Looking at the time-averaged temperature contour, it can be seen that the highest temperature was found both along the central axis of the burner and in the external recirculation, where the hot gases were trapped and recirculate interacting with the flame, burning again. A different wall behaviour was observed in LES or in RANS simulations. In LES, unburned gases burn before reaching the burner wall, while in RANS simulations combustion occurred closer to the wall. The instantaneous field of the Heat Release Rate (HRR) was also shown in Fig. 6 to clearly show the flame morphology and the flame front. It was observed how one of the key factor of the approach to the wall was attributed to the constant A in Eq. 3, since it was directly proportional to the speed of the turbulent flame, U_t, and greatly influences it. After a sensitivity study, the value of constant A=0.8 was found to be the one that best captured the flame behaviour, having as reference OH chemiluminescence values, shown by Meloni et al. (2023). To get a preliminary idea of the differences in terms of flow and temperature fields, a comparison of axial velocity (Fig. 7a) and temperature (Fig. 7b) contours between the investigated RANS turbulence models was shown in Fig. 7.

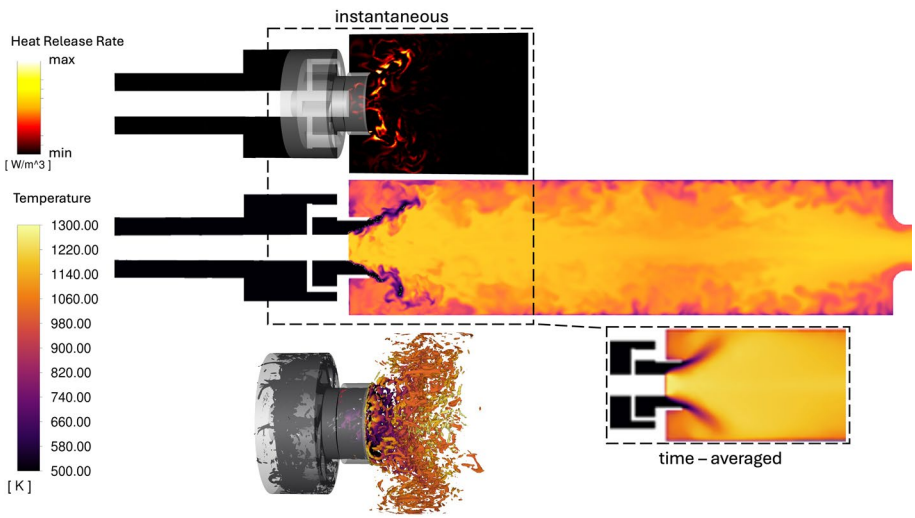

Fig. 6 Instantaneous and time-averaged temperature and Heat Release Rate fields derived by LES (Dynamic Smagorinsky-Lilly). The instantaneous iso-surface of progress variable = 0.9 was colored by the temperature

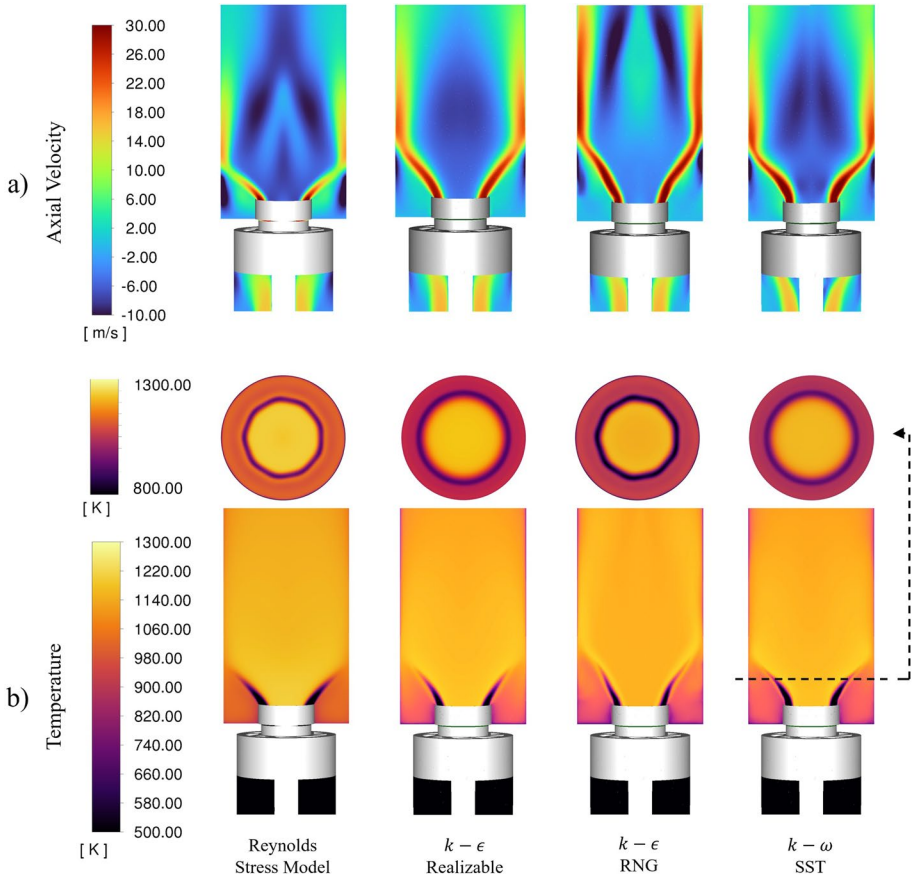

Fig. 7 Axial velocity **a** and temperature **b** fields of the different RANS turbulence models investigated

In terms of axial velocity, there was a non-negligible difference in the recirculation zones: the Realizable and RNG k-ϵ models have a single inner recirculation zone, IRZ, whereas in the k-ω SST and RSM models the IRZ was divided into two different central zones, which was consistent with the LES simulation, shown in Fig. 5. The external recirculation zone, ERZ, was similar for all turbulence models here analysed. The k-ϵ RNG model differed from other models because it exhibited higher axial wall velocity along the walls. However, for all RANS models, the average axial velocity along the wall was approximately 7 m/s higher than for LES simulations, specifically resulted in -8 m/s and -15 m/s, respectively, in the flame region. In terms of temperature, all models succeed in capturing the behaviour of the flame. However, close to the wall and along the centreline, the RSM model has a similar temperature value to that estimated by LES, due to the fact that RSM directly calculate the components of the specific Reynolds stress tensor by solving their governing transport equations; in fact, temperature was higher than the other models tested in those zones. To better highlight the temperature variation near the wall, additional contours along a plane located at x = 1D were added to Fig. 7 for each of the simulations presented. Additionally, the temperature scale was narrowed to more effectively capture these differences. In the following sections, axial

velocity and temperature profiles are also provided to offer a more detailed analysis of this variation.

Figure 8 shows the instantaneous and time-averaged axial velocity and temperature fields for LES with the Dynamic Smagorinsky-Lilly and WALE models and Reynolds Stress Model in two different planes perpendicular to the flow at x=1D and x=4D. The two LES models do not differ substantially in terms of both axial velocity and temperature; it is only noticeable that the axial velocity of the Smagorinsky-Lilly model is 2 m/s higher than that of the WALE model in the plane at x=1D, while the two fields are almost equal at x=4D. Meanwhile, the Reynolds Stress model shows an underestimation of the axial velocity at x=1D in comparison to the LES models with no positive velocity along the centreline, while for x=4D there is an overestimation of the axial velocity on the walls. The behavior of the axial and tangential components of the flow along the combustor, particularly the reduction of the downstream peak, can be correlated with the swirl decay observed experimentally by Kitoh et al. (Kitoh (1991)), who demonstrated that the swirl intensity in turbulent flows decreases exponentially along the axial direction due to wall friction. Regarding the temperature field, the two LES simulations differ by about 25 K with a higher temperature observed by the Smagorinsky-Lilly model. As for axial velocity, the Reynolds Stress model also underestimates the temperature field, both at x=1D and x=4D.

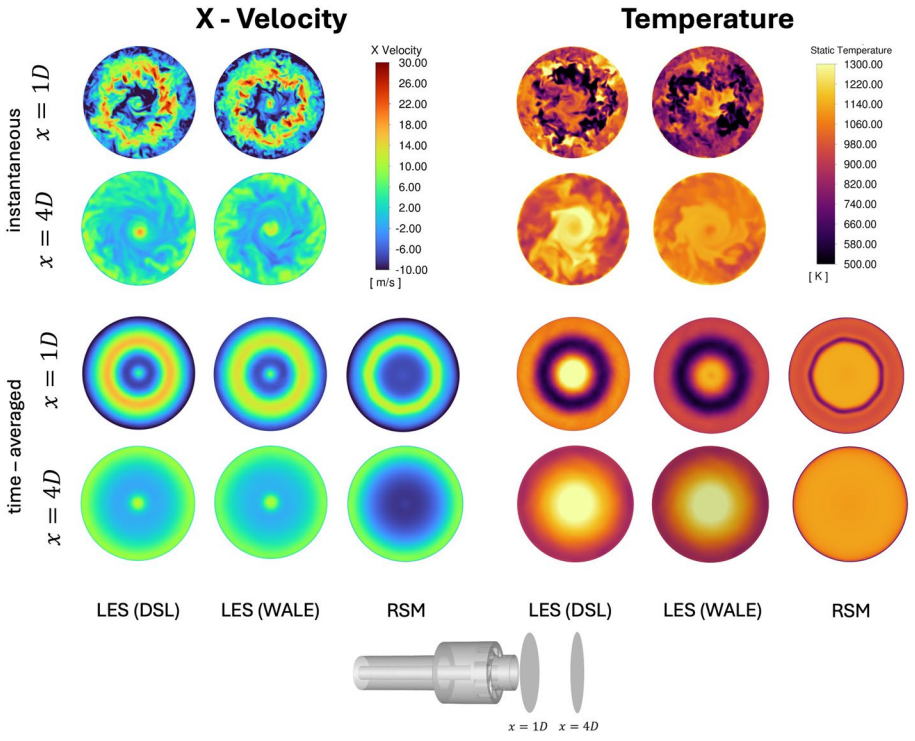

Fig. 8 Instantaneous and time-averaged axial velocity and temperature fields comparison at x=1D and x=4D for LES (DSL), LES (WALE) and Reynolds Stress models

In Fig. 9, a comparative analysis of axial velocity and temperature profiles was shown across various turbulence models at different locations within the domain, specifically at x=1D and x=4D. Notably, distinct trends among the models emerge, revealing similarities in velocity and temperature distributions. Since no PIV data were available, the profiles derived from the LES simulations were taken as a reference for the turbulence models, due to the higher accuracy in terms of NO_x and exhaust temperature. Regarding the axial velocity, a noticeable difference can be seen along the central axis of the burner, where the profile derived from the LES model there was a positive value, in both planes x=1D (Fig. 9a) and x=4D (Fig. 9c). The profile was only predicted by the RSM model at x=1D, while for the other RANS models the central recirculation (IRZ) was not divided into two separate portions. In particular, the RSM model showed higher accuracy due to its ability to estimate complex flows thanks to the additional transport equations. The 7-equations of RSM is able to capture the anisotropy of turbulence and characterize the recirculation zones. The near wall velocity was similar among all RANS models while it results in a negative axial velocity for the LES model. In addiction, the axial velocity profile derived from the LES averaged field was smoother than the other turbulence models, especially in

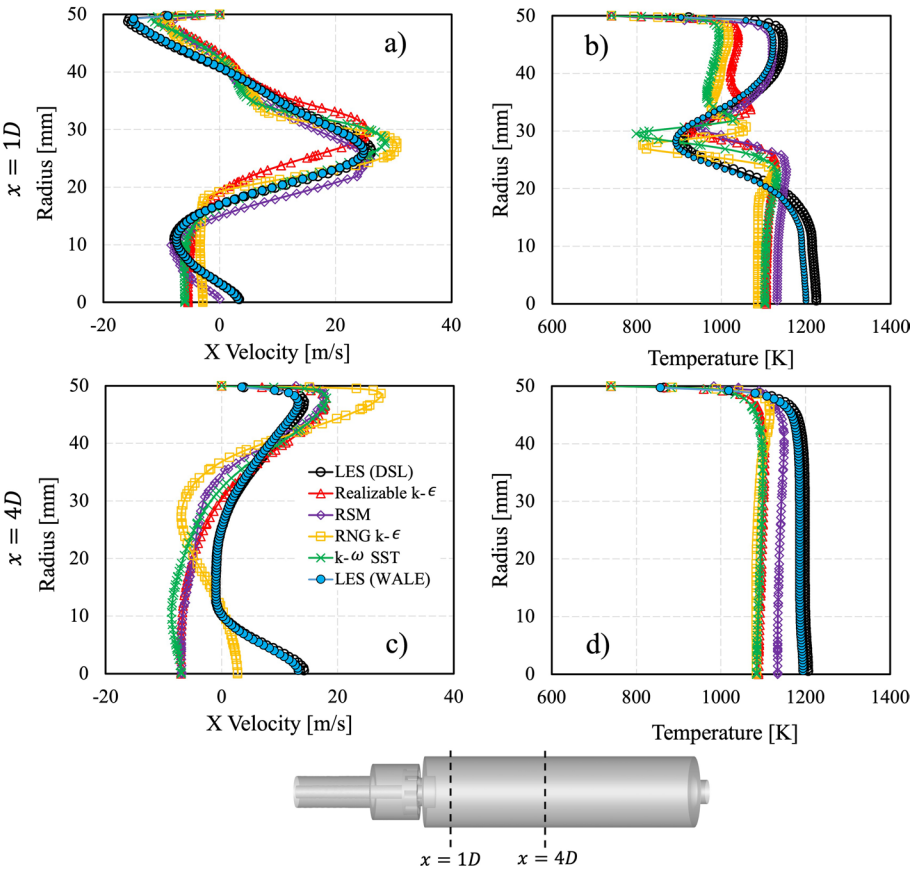

Fig. 9 Axial velocity and temperature profiles comparison between the turbulence models analysed at x=1D and x=4D

Table 4 A comparison between the results derived from the experimental campaign and the numerical analysis on emissions and exhaust temperature

	Exp.	LES(DSL)	LES(WALE)	RSM	k-ω SST	Real. k-ϵ	RNG k-ϵ
NO_x [*ppmvd*]	2761	2511.5	2385.9	1950.2	1661.33	1571.8	1747.5
Exh. Temp. [*K*]	963	978	977	976	974	974	975

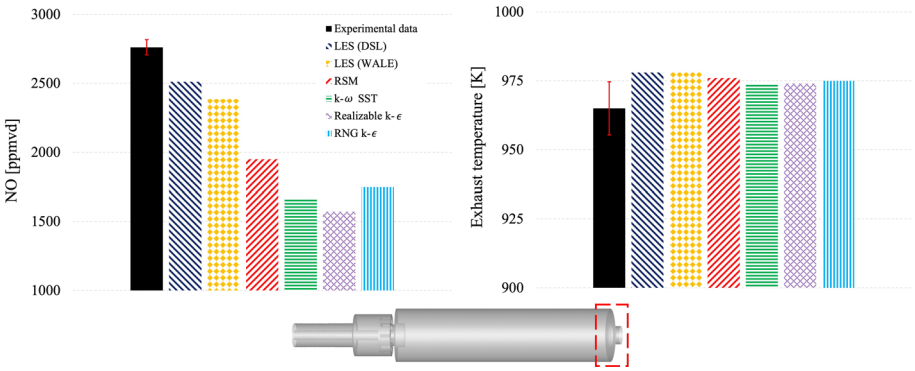

Fig. 10 NO emissions and exhaust temperature results derived by numerical simulations and compared with experimental data

the range 30 mm $\leq$ y $\leq$ 50 mm (see Fig. 9a). The axial velocity was over predicted by RNG $k-\epsilon$ model; this was noticeable both within the flame front (Fig. 9a) and in the near-wall at x=4D (Fig. 9c), since this turbulence model is not able to accurately predict the central recirculation zone generated by vortex breakdown bubble instability (Safavi and Amani (2018)).

A comparison between temperature profiles were shown in Figs. 9b,d. As before, the LES profile shows a greater temperature gradient along the burner's longitudinal axis. In the RANS the flame front was narrower than in the LES. The temperature reached by the LES resulted 100 *K* higher than the other models in the flame zone and near the walls. The same temperature gap was present at x=4D, where the trend was maintained but underestimation by the RANS simulations was present. As for velocity, the temperature derived by RNG $k-\epsilon$ model differed more from the others models, in particular underestimating its value in unburnt zone, as shown in Fig. 9b. The deviation of the RANS models from the experimental emissions data could be attributed to the fact that RANS cannot capture the details of the phenomena without careful calibration. It can only be predicted by the RSM model, which takes into account the effects of Reynolds stresses, for a more accurate analysis of swirl phenomena; NO_x emissions are characterised by a slow chemical reaction and need transient simulations for higher accuracy. A similarity in terms of velocity and temperature profiles can be seen between the k-ϵ Realizable and k-ω SST models, with a single difference in terms of axial velocity at x=4D. The emission results and the exhaust temperature derived from the different turbulence models analysed were shown in Table 4, comparing them with the data derived from the experimental campaign (Mazzotta et al. (2024)). The emission results were further illustrated in Fig. 10. It was found that the emission and exhaust temperature predictions of the Large Eddy Simulations models were in agreement with the experimental data when considering the error bar,

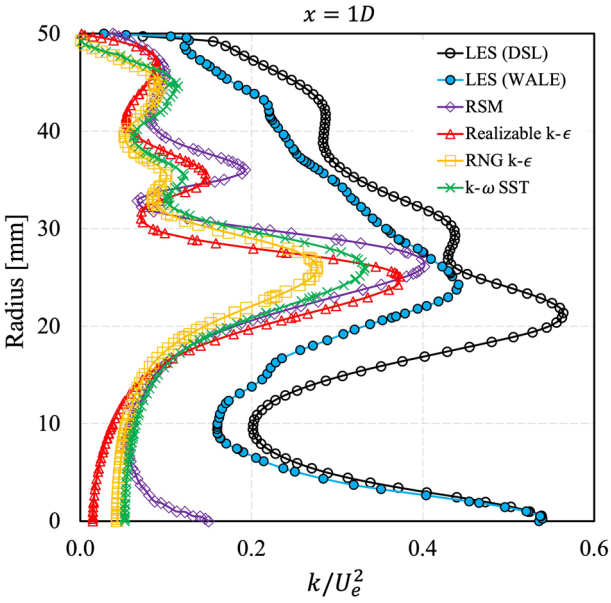

Fig. 11 Normalized turbulent kinetic energy distribution of different turbulence models at x=1D

with small errors given by the LES with the Smagorinsky-Lilly model, with an error less than 10% and 3% respectively, despite a combustion model not based on detailed chemistry. On the RANS side, the results showed that the Reynolds Stress Model was the most accurate in predicting NO_x emissions among the RANS models, even if the error was not negligible. With regard to the temperature at the combustor outlet, all RANS simulations predicted a value, similar to the LES one, validating the CFD model against the experimental data, resulting in a error less than 3%.

3.1 Turbulent Kinetic Energy, Reynolds Shear Stress

The properties of the fluctuating velocity field and transport phenomena were analyzed through the turbulence kinetic energy (k) and the Reynolds shear stresses ($\overline{u'v'}$, $\overline{u'w'}$, $\overline{v'w'}$). The turbulent kinetic energy represents the energy associated with turbulent motions per unit mass and was measured as:

$$k_{res} = \frac{1}{2}\left(\overline{u'u'} + \overline{v'v'} + \overline{w'w'}\right) \tag{7}$$

where $u'u'$, $v'v'$, and $w'w'$ are the components of the velocity fluctuation variances in the x, y, and z directions, respectively. These fluctuation values were derived from the Reynolds decomposition, where the velocity field is split into a mean and fluctuating part (Adrian et al. (2000)). In the context of RANS simulations using the k-ϵ or k-ω turbulence models, the turbulent kinetic energy (k) is calculated by solving a specific transport equation and modeled using the Boussinesq hypothesis. In LES, the velocity fluctuations were obtained through statistical averaging of the resolved flow field over 6 Flow Through Time (FTT). The filtered components $\overline{u'u'}$, $\overline{v'v'}$, and $\overline{w'w'}$ were collected and used to compute the turbulent kinetic energy. The Reynolds Stress Model (RSM) explicitly resolves the

Reynolds stresses $\overline{u'v'}$, $\overline{u'w'}$, and $\overline{v'w'}$, allowing for direct computation of the Reynolds shear stresses. Figure 11 presents the radial distribution of the normalized turbulent kinetic energy (k/U_e^2), where U_e^2 is the inlet velocity, at a downstream location corresponding to $x = 1D$. The turbulence models investigated in this work are compared to assess their accuracy in predicting the turbulence intensity across the radial profile. Along the centreline region, where y≤ 10 mm, the LES models predict the highest values of k, with the DSL model exhibiting the largest peak. The WALE model follows closely, providing a slightly lower prediction of turbulence near the centreline. These results from LES are generally regarded as the most accurate due to their superior ability to resolve large-scale turbulence.

The RSM model demonstrates a noticeable improvement over the RANS models in this region, though it still does not match the accuracy of the LES predictions; the RANS models significantly underpredict the turbulent kinetic energy near the centreline, exhibiting large deviations from the LES results. In the flame region, where 10≤ y≤30, notable differences between the models emerge: while the LES models continue to predict higher turbulence levels, the RSM model shows more comparable results to the LES models, providing a better prediction than any of the RANS models. However, the RSM still has some discrepancies, displaying fluctuations that are absent in the LES data. The RANS models exhibit relatively close agreement with one another, yet they collectively underestimate the turbulent kinetic energy in this region. As for the centreline, across the wall the LES models predict the highest turbulent kinetic energy, while RANS models underpredict the turbulent kinetic energy. Figure 12 shows the radial distribution of normalized Reynolds shear stresses (from left to right, $\overline{u'v'}/U_e^2$, $\overline{u'w'}/U_e^2$, $\overline{v'w'}/U_e^2$) at a $x = 1D$. This figure focuses on a comparison between the LES and RSM models. Similarities can be observed between the components $\overline{u'v'}$ and $\overline{u'w'}$ due to the nature of the analyzed flow; however, only in the LES (WALE) model is a lower value observed in the $\overline{u'w'}$ component. Similarly to turbulent kinetic energy, the LES models predict significantly higher Reynolds shear stresses compared to the RSM, which continues to underestimate the shear stresses, failing to capture the broader shear layer interactions, mainly along the centreline. The peak occurs where 15 ≤ y ≤ 25, with the LES (DSL) model showing the highest values across all three components analyzed.

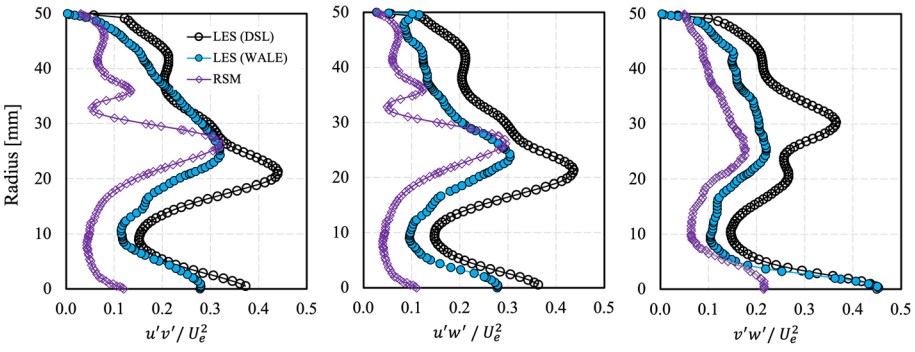

Fig. 12 Radial distribution of normalized Reynolds shear stresses at a x=1D

4 Conclusion

The impact of the turbulence models were investigated in gas turbine system fed with ammonia-hydrogen blend and compared with experimental data in terms of NO_x emissions and exhaust temperature. Two different sub-grid models in high-fidelity LES and four RANS turbulence models were analysed; in particular, the Smagorinsky-Lilly and WALE models were evaluated on the LES side, while the Realizable k-ϵ, RNG k-ϵ, k-ω SST and Reynolds Stress (RSM) models were compared on the RANS side. Numerical simulations were developed using a tabulated chemistry approach with a detailed chemical scheme that takes into account all NO_x reactions. The main outcomes of this work can be summarized as follows:

- The LES results, which takes into account residence times of slow species such as NO and NO_2 with greater accuracy, were in good agreement with experimental data based on NO_x emissions and exhaust temperature, when compared with the RANS models based on the resolution of the averaged Navier–Stokes equations.
- The two LES sub-grid models investigated and compared do not differ significantly in terms of both axial velocity and temperature.
- For the axial velocity field a non-negligible difference in the recirculation zones was observed for all RANS simulations when compared with LES ones (time-averaged). In particular, the Realizable and RNG k-ϵ models have a single zone of internal recirculation, IRZ, while the k-ω SST and RSM models show the IRZ divided into two different zones, in agreement with the LES. On the other hand, the external recirculation zone, ERZ, was similar for all turbulence models analysed.
- Regarding the temperature field, all turbulence models were able to capture the behaviour of the flame. However, close to the wall and along the centreline, the RSM model gives a temperature value in agreement with LES, thanks to the directly calculation of the specific Reynolds stress tensor components by solving their governing transport equations. This becomes particularly relevant when swirling flows are to be considered through Eddy-Viscosity RANS models, which require additional calibrations.
- Despite the averaged nature of the RANS approach, the exhaust temperature was well predicted by all turbulence models and in agreement with experimental data.
- The calibration of the turbulence-chemistry interaction model was a valid strategy to emulate the combustion process and the morphology of ammonia/hydrogen flames. In particular, the calibration of the constant A in Eq. 3 resulted to be crucial to accurate predict the turbulent flame speed, U_t.
- The addition of the scalar transport equations of the species characterising NO_x emissions is highly recommended, particularly when applied to LES coupled with FGM. Nevertheless, the NO_x emissions estimated by the RANS approach resulted in a non-negligible error compared to the experimental data. However, the RSM has a smaller error than the turbulence models based on 2 equations. Due to the formation of slow species such as NO and NO_2, a unsteady model appears to be necessary.
- The computational times required by the LES are 8 times greater than for the k-ϵ (Realizable and RNG) and k-ω SST models, and 5 times greater than the RSM model. Due to the high computational cost of LES, a good compromise may be to use RSM, which showed a good prediction of the velocity and temperature fields, but a more accurate combustion model is needed that takes into account the nature of slow species for the prediction of NO_x emissions.

- The high-fidelity LES model added useful numerical information for the analysis of the combustion process not available from experimental data, such as the velocity field, temperature difference in the different burner regions, velocity and temperature behaviour in wall and recirculation zones.
- The RANS models underpredict turbulent kinetic energy and Reynolds shear stress, especially in the critical regions near the centreline and in the flame zone. Among them, the RSM models show better agreement with the LES results but they still exhibit significant errors relative to LES.

Acknowledgements This research is supported by the Ministry of University and Research (MUR) as part of the PON 2014–2020 "Research and Innovation" resources - Green/Innovation Action (DM MUR 1061/2021 and DM MUR 1062/2021) and part of the European Union program NextGenerationEU, PNRR - M4C2 - ECS-00000024 "Rome Technopole". Data reported in this paper have been gathered within the project Flex&Confu, funded by the European Union, which is gratefully acknowledged. The authors would like to acknowledge the Cardiff University Gas Turbine Research Centre and Steve Morris for the support in the experimental campaign.

Author Contributions **L. Mazzotta**: Conceptualization, Methodology, Software, Writing – original draft, Visualization. **R. Lamioni**: Software, Methodology, Writing – original draft. **G. Agati**: Methodology, Review & editing. **A. Evangelisti**: Software, Review & editing. **F. Rispoli**: Review & editing, Supervision. **A. Valera-Medina**: Review & editing, Supervision. **D. Borello**: Review & editing, Supervision.

Funding Open access funding provided by Università degli Studi di Roma La Sapienza within the CRUI-CARE Agreement. This work has been funded by Ministry of University and Research (MUR) as part of the PON 2014–2020 "Research and Innovation" resources - Green/Innovation Action (DM MUR 1061/2021 and DM MUR 1062/2021) and part of the European Union program NextGenerationEU, PNRR - M4C2 - ECS-00000024 "Rome Technopole". Data reported in this paper have been gathered within the project Flex&Confu, funded by the European Union.

Declarations

Conflict of interest The authors declare that they have no known competing financial interests or personal relationships that could have appeared to influence the work reported in this paper.

References

Adrian, R., Christensen, K., Liu, Z.C.: Analysis and interpretation of instantaneous turbulent velocity fields. Exp. Fluids **29**, 275–290 (2000). https://doi.org/10.1007/s003489900087

Alnasif, A., Mashruk, S., Hayashi, M., et al.: Performance investigation of currently available reaction mechanisms in the estimation of NO measurements: a comparative study. Energies (2023). https://doi.org/10.3390/en16093847

Ansari, N., Orsino, S., Meloni, R., et al.: Large-eddy simulation of a non-premixed ammonia-hydrogen flame: Nox emission and flame characteristics validation. In: Proceedings of ASME Turbo Expo 2024

Volume 3B: Combustion, Fuels, and Emissions:V03BT04A073. https://doi.org/10.1115/GT2024-129248 (2024)

Castellani S, Nassini PC, Andreini A, et al: Numerical Modelling of Swirl Stabilised Lean-Premixed H_2-CH_4 Flames With the Artificially Thickened Flame Model. In: Proceedings of ASME Turbo Expo 2023 Volume 3A: Combustion, Fuels, and Emissions. https://doi.org/10.1115/GT2023-101994 (2023)

Castellani, S., Nassini, P.C., Andreini, A., et al.: Numerical modeling of swirl stabilized lean-premixed h2-ch4 flames with the artificially thickened flame model. J. Eng. Gas Turbines Power **146**(6), 061019 (2024). https://doi.org/10.1115/1.4063829

Chiong, M.C., Chong, C.T., Ng, J.H., et al.: Advancements of combustion technologies in the ammonia-fuelled engines. Energy Convers. Manage. **244**, 114460 (2021). https://doi.org/10.1016/j.enconman.2021.114460

da Rocha, R.C., Costa, M., Bai, X.S.: Chemical kinetic modelling of ammonia/hydrogen/air ignition, premixed flame propagation and no emission. Fuel **246**, 24–33 (2019). https://doi.org/10.1016/j.fuel.2019.02.102

Flohr PDI, Pitsch H (2001) A turbulent flame speed closure model for les of industrial burner flows. In: Proceed. summer program

Füzesi, D., Józsa, V., Csemány, D.: Numerical investigation on the effect of hydrogen share in NH_3/H_2 blends in a turbulent lean-premixed swirl burner. Int. J. Hydrogen Energy **49**, 816–827 (2024). https://doi.org/10.1016/j.ijhydene.2023.09.091

Germano, M., Piomelli, U., Moin, P., et al.: A dynamic subgrid-scale eddy viscosity model. Phys. Fluids A **3**(7), 1760–1765 (1991). https://doi.org/10.1063/1.857955

Goodwin, D.G., Moffat, H.K., Schoegl, I., et al.: Cantera: an object-oriented software toolkit for chemical kinetics, thermodynamics, and transport processes. Zenodo (2022). https://doi.org/10.5281/zenodo.6387882

Hanjalić, K., Launder, B.E.: A Reynolds Stress Model of turbulence and its application to thin shear flows. J. Fluid Mech. **52**(4), 609–638 (1972). https://doi.org/10.1017/S002211207200268X

Ilbas, M., Yılmaz, İlker, Kaplan, Y.: Investigations of hydrogen and hydrogen-hydrocarbon composite fuel combustion and NOx emission characteristics in a model combustor. Int. J. Hydrogen Energy **30**(10), 1139–1147 (2005). https://doi.org/10.1016/j.ijhydene.2004.10.016

Kitoh, O.: Experimental study of turbulent swirling flow in a straight pipe. J. Fluid Mech. **225**, 445–479 (1991)

Kobayashi, H., Hayakawa, A., Somarathne, K.K.A., et al.: Science and technology of ammonia combustion. Proc. Combust. Inst. **37**(1), 109–133 (2019). https://doi.org/10.1016/j.proci.2018.09.029

Li, Z., Li, S.: Kinetics modeling of NOx emissions characteristics of a NH_3/H_2 fueled gas turbine combustor. Int. J. Hydrogen Energy **46**(5), 4526–4537 (2021). https://doi.org/10.1016/j.ijhydene.2020.11.024

Magnussen, B.: On the structure of turbulence and a generalized eddy dissipation concept for chemical reaction in turbulent flow. In: 19th aerospace sciences meeting (1976)

Mashruk, S., Xiao, H., Pugh, D., et al.: Numerical analysis on the evolution of NH_2 in ammonia/hydrogen swirling flames and detailed sensitivity analysis under elevated conditions. Combust. Sci. Technol. **195**(6), 1251–1278 (2023). https://doi.org/10.1080/00102202.2021.1990897

Mashruk, S., Shi, H., Mazzotta, L., et al.: Perspectives on nox emissions and impacts from ammonia combustion processes. Energy & Fuels (2024). https://doi.org/10.1021/acs.energyfuels.4c03381

Mazzotta, L., Lamioni, R., D'Alessio, F., et al.: Modeling ammonia-hydrogen-air combustion and emission characteristics of a generic swirl burner. J. Eng. Gas Turbines Power (2024). https://doi.org/10.1115/1.4064807

Meloni R, Babazzi G, Castellani S, et al: Investigation of the Pressure Effect onto the NOx Emission of a Perfectly Premixed NH_3-H_2 Flame Through the Validation of a Thickened Flame Model. Proc of the European Comb Meeting. (2023)

Meloni R, Mazzotta L, Pucci E, et al: Large Eddy Simulations for the Prediction of Fuel-Bound NOx Emissions: Application to NH_3 and NH_3-CH_4 Blends at Different Operating Conditions. Proceedings of ASME Turbo Expo 2024 Volume 3A: Combustion, Fuels, and Emissions. (2024) https://doi.org/10.1115/GT2024-123875

Menter, F.R.: Two-equation eddy-viscosity turbulence models for engineering applications. AIAA J. **32**(8), 1598–1605 (1994). https://doi.org/10.2514/3.12149

Nicoud, F., Ducros, F.: Subgrid-scale stress modelling based on the square of the velocity gradient tensor. Flow Turbul. Combust. **62**, 183–200 (1999). https://doi.org/10.1023/A:1009995426001

Oijen, J.V., Goey, L.D.: Modelling of premixed laminar flames using flamelet-generated manifolds. Combust. Sci. Technol. **161**(1), 113–137 (2000). https://doi.org/10.1080/00102200008935814

Otomo, J., Koshi, M., Mitsumori, T., et al.: Chemical kinetic modeling of ammonia oxidation with improved reaction mechanism for ammonia/air and ammonia/hydrogen/air combustion. Int. J. Hydrogen Energy **43**(5), 3004–3014 (2018). https://doi.org/10.1016/j.ijhydene.2017.12.066

Ouali, S.: Numerical simulation of H_2 addition effect to CH_4 Premixed turbulent flames for gas turbine burner. J. Appl. Fluid Mech. **17**(8), 1746–1758 (2024). https://doi.org/10.47176/jafm.17.8.2466

Pope, S.B.: Turbulent flows. Cambridge University Press (2000)

Pope, S.B.: Ten questions concerning the large-eddy simulation of turbulent flows. New J. Phys. **6**(1), 35 (2004). https://doi.org/10.1088/1367-2630/6/1/035

Pugh, D., Bowen, P., Valera-Medina, A., et al.: Influence of steam addition and elevated ambient conditions on NOx reduction in a staged premixed swirling NH3/H2 flame. Proc. Combust. Inst. **37**(4), 5401–5409 (2019). https://doi.org/10.1016/j.proci.2018.07.091

Runyon, J., Marsh, R., Bowen, P., et al.: Lean methane flame stability in a premixed generic swirl burner: Isothermal flow and atmospheric combustion characterization. Exp. Therm. Fluid Sci. **92**, 125–140 (2018). https://doi.org/10.1016/j.expthermflusci.2017.11.019

Safavi, M., Amani, E.: A comparative study of turbulence models for non-premixed swirl-stabilized flames. J. Turbul. **19**(11–12), 1017–1050 (2018). https://doi.org/10.1080/14685248.2018.1527033

Smagorinsky, J.: General circulation experiments with the primitive equations: I. The basic experiment. Monthly Weather Rev. **91**(3), 99–164 (1963)

Valera-Medina, A., Xiao, H., Owen-Jones, M., et al.: Ammonia for power. Prog. Energy Combust. Sci. **69**, 63–102 (2018). https://doi.org/10.1016/j.pecs.2018.07.001

Van Oijen, J., de Goey, L.: Modelling of premixed laminar flames using flamelet-generated manifolds. Combust. Sci. Technol. **161**(1), 113–137 (2000). https://doi.org/10.1080/00102200008935814

Wilcox, D.: Turbulence Modeling for CFD. Anaheim, DCW Industries (1998)

Xiao, H., Valera-Medina, A.: Chemical kinetic mechanism study on premixed combustion of ammonia/hydrogen fuels for gas turbine use. J. Eng. Gas Turbines Power (2017). https://doi.org/10.1115/1.4035911

Yakhot, V., Orszag, S.A., Thangam, S., et al.: Development of turbulence models for shear flows by a double expansion technique. Phys. Fluids A **4**(7), 1510–1520 (1992). https://doi.org/10.1063/1.858424

Yang, S.L., Siow, Y.K., Peschke, B.D., et al.: numerical study of nonreacting gas turbine combustor swirl flow using reynolds stress model. J. Eng. Gas Turbines Power **125**(3), 804–811 (2003). https://doi.org/10.1115/1.1560706

Zeldovich Y.: The oxidation of nitrogen in combustion explosions. Acta Physicochimica USSR (1946)

Zimont, V., Polifke, W., Bettelini, M., et al.: An efficient computational model for premixed turbulent combustion at high reynolds numbers based on a turbulent flame speed closure. J. Eng. Gas Turbines Power **120**(3), 526–532 (1998). https://doi.org/10.1115/1.2818178

Authors and Affiliations

Luca Mazzotta[1,2] · Rachele Lamioni[3] · Giuliano Agati[4] · Adriano Evangelisti[1] · Franco Rispoli[4] · Agustin Valera-Medina[5] · Domenico Borello[4]

✉ Luca Mazzotta
luca.mazzotta@uniroma1.it

✉ Rachele Lamioni
rachele.lamioni@unipi.it

Giuliano Agati
giuliano.agati@uniroma1.it

Adriano Evangelisti
adriano.evangelisti@uniroma1.it

Franco Rispoli
franco.rispoli@uniroma1.it

Agustin Valera-Medina
valeramedinaA1@cardiff.ac.uk

Domenico Borello
domenico.borello@uniroma1.it

[1] Department of Astronautical, Electrical and Energetic Engineering, Sapienza University of Rome, Via Eudossiana 18, 00184 Rome, Italy

[2] Baker Hughes, Via Felice Matteucci, 2, 50127 Florence, Italy

[3] Department of Industrial and Civil Engineering, University of Pisa, L.go L. Lazzarino, 56122 Pisa, Italy

[4] Department of Mechanical and Aerospace Engineering, Sapienza University of Rome, Via Eudossiana 18, 00184 Rome, Italy

[5] College of Physical Sciences and Engineering, Cardiff University, Cardiff CF24 3AA, UK